BAREKENG: Journal of Mathematics and Its Applications
December 2026 Volume 20 Issue 4 Page 3391-3404
P-ISSN: 1978-7227 E-ISSN: 2615-3017
https://doi.org/10.30598/barekengvol20iss4pp3391-3404

BASIC-STATE ANALYSIS OF NANOFLUID BIOCONVECTION WITH GYROTACTIC MICROORGANISMS UNDER ZERO-NANOPARTICLE FLUX BOUNDARY CONDITION

Ming Hui Lim [1], **Yian Yian Lok** [2*], **Syakila Ahmad** [3], **Norshafira Ramli** [4], **Anuar Ishak** [5]

[1,2]*Mathematics Section, School of Distance Education, Universiti Sains Malaysia.*
[3,4]*School of Mathematical Sciences, Universiti Sains Malaysia*
USM Penang, 11800, Malaysia.

[5]*Department of Mathematical Sciences, Faculty of Science and Technology, Universiti Kebangsaan Malaysia*
UKM Bangi, 43600, Malaysia.

*Corresponding author's e-mail: * **lokyy@usm.my***

Article Info

Article History:
Received: 21st October 2026
Revised: 28th April 2026
Accepted: 07th June 2026
Available online: 24th August 2026

Keywords:
Basic-state solution;
Finite-depth layer;
Gyrotactic microorganisms;
Nanofluid bioconvection;
Zero-nanoparticle flux boundary conditions.

ABSTRACT

This study presents an analysis of the basic state of nanofluid bioconvection in a horizontal finite-depth layer containing gyrotactic microorganisms. To enhance the physical realism of the system, zero-nanoparticle flux boundary conditions are incorporated for the nanoparticle fraction. The basic-state solution refers to a simplified, time-independent configuration that serves as the reference or background state for analysing perturbations in stability analysis. In this case, the quiescent flow has zero velocity, while other state variables - such as temperature, nanoparticle concentration, and microorganism density - vary only in the vertical direction. The resulting system of ordinary differential equations is solved to obtain analytical solutions while the effects of key parameters on the steady-state profiles are investigated. The results show that the swimming strength parameter mainly influences microorganism accumulation near the upper boundary. Both the swimming strength parameter and the bioconvection Rayleigh number have only a limited effect on the pressure profile. In contrast, the thermal Rayleigh number and modified diffusivity ratio produce the most noticeable pressure variations, indicating that thermal and thermophoretic effects play the dominant role in shaping the basic-state pressure distribution. Overall, the pressure profile remains nearly linear. The findings provide insight into the role of zero-nanoparticle flux boundary conditions in finite-depth nanofluid bioconvection systems.

How to cite this article:

M. H. Lim, Y. Y. Lok, S. Ahmad, N. Ramli and A. Ishak., "BASIC-STATE ANALYSIS OF NANOFLUID BIOCONVECTION WITH GYROTACTIC MICROORGANISMS UNDER ZERO-NANOPARTICLE FLUX BOUNDARY CONDITION", *BAREKENG: J. Math. & App.*, vol. 20, no. 4, pp. 3391-3404, Dec, 2026.

Journal homepage: *https://ojs3.unpatti.ac.id/index.php/barekeng/*
Journal e-mail: *barekeng.math@yahoo.com; barekeng.journal@mail.unpatti.ac.id*

Research Article · Open Access

1. INTRODUCTION

Bioconvection arises from hydrodynamic instabilities caused by the biased swimming of microorganisms, leading to the formation of motion patterns [1]. Hydrodynamic instabilities primarily arise from the accumulation of microbial cells with varying buoyancy, which results in inconsistent density distributions, or from the interaction between an unstable fluid velocity field and cell concentration. First observed in the 19th century [2], the term “bioconvection” was introduced by Platt in 1961 [3]. Hill et al. [4] developed the foundational model for bioconvection in gyrotactic suspensions, considering dilute suspensions of motile microorganisms influenced by gravitational torque and viscous resistance in a finite depth layer. They formulated governing equations and performed a linear stability analysis to investigate flow characteristics and the onset of instability. Today, it remains an active research area in numerical heat transfer, with applications in bioreactors [5], biofuel production [6], and microfluidic devices [7].

Nanofluids, which are suspensions of nanoparticles in base fluids such as water, offer enhanced thermophysical properties over conventional fluids. Choi and Eastman [8] introduced this concept, followed by two key models: Tiwari and Das [9], emphasizing the nanoparticle volume fraction, and Buongiorno [10], focusing on two major slip mechanisms, which are thermophoresis and Brownian motion. Nield and Kuznetsov’s [11] incorporated the Buongiorno model in their studies on nanofluid natural convection studies. Kuznetsov [12] further extended this framework of Nield and Kuznetsov [11] by introducing gyrotactic microorganisms, adapting Hill et al.’s model [4]. These progressive developments have significantly advanced the understanding of nanofluid dynamics and their applications in heat transfer enhancement.

Since the emergence of the nanofluid bioconvection model, numerous studies have explored various physical effects and boundary conditions based on this framework. More recent research has further advanced it by incorporating variable-viscosity fluids such as third-grade nanofluid [13], Carreau [14], Cross [15], Sutterby [16], [17], Eyring-Powell [18], [19], micropolar [20], Williamson [21], Casson [22], Jeffrey [23], Oldroyd-B fluids [24], Maxwell [25], [26] and Darcy-Forchheimer porous medium [27]. It is important to note that all the aforementioned studies typically considered a fluid domain with a sufficiently large (effectively infinite) depth. Such configuration is easier to analyse due to the applicability of boundary layer approximations and the use of similarity transformations in the governing equations.

In contrast to infinite-depth layers, some studies have also investigated finite-depth configurations, accounting for factors such as small particles [28], [29], thermo-bioconvection [30], [31], vertical vibration [32], [33], inclined temperature gradient [34], and magnetic field [35], [36]. The consideration of a finite-depth domain is more practical than the infinite-depth setting, as it more accurately reflects real-world applications, particularly in biofuel cultivation systems, which involve open and stagnant biofuel ponds with shallow depths. Unlike open flow studies, finite-depth configurations require a different approach that involves directly solving the system for the basic steady-state profile before performing stability analysis. The steady state profile serves as the base state for introducing small perturbations in the linearised system. The onset of bioconvection in finite-depth geometries is typically analysed using linear stability theory, employing methods like Galerkin approximations [28], [30], [31], [32], [33], collocation [34], and Chebyshev pseudospectral techniques [35], [36] to estimate critical Rayleigh numbers. More recently, nonlinear models such as the Lorenz approach [37] have been used to understand the chaotic behaviour in gyrotactic bioconvection. Avramenko et al. [38] revisited Hill et al.’s model [4], applied the Lorenz approach to explore low-dimensional dynamics.

Despite these advances, a comprehensive analytical treatment of the basic state for nanofluid bioconvection in a finite-depth layer under zero-nanoparticle flux boundary conditions is still lacking. Kuznetsov [12] extended the nanofluid convection model of Nield and Kuznetsov [11] by incorporating gyrotactic microorganisms, thereby establishing a nanofluid bioconvection framework, but no basic-state analysis was presented in these studies. Subsequently, Kuznetsov [39], also developed based on [12], examined a case involving two different species of microorganisms. However, the basic-state analysis was only brief, since the main emphasis of [39] was on linear stability analysis. Hence, there remains a need for a dedicated analytical study of the basic-state profiles, on extending the work of Kuznetsov [12] under the revised zero-nanoparticle flux boundary conditions introduced by Nield and Kuznetsov [40].

Motivated by this gap, the present study investigates the basic state of nanofluid bioconvection in a horizontal finite-depth layer containing gyrotactic microorganisms under the zero-nanoparticle flux boundary conditions proposed by Nield and Kuznetsov [40]. Despite the strong recent emphasis on open-flow problems, finite-depth analysis remains relevant and has continued to appear in recent studies [35, 36]. Its continued interest arises not only from physical considerations, but also from its mathematical significance in clarifying the structure of coupled transport processes in bounded configurations. In this study, the governing equations are transformed into a nondimensional form using appropriate characteristic scales. Under the assumption of a quiescent base state, steady-state solutions are derived analytically. The influence of key physical parameters on the pressure profile is then analysed in detail. The results provide physical insight into the relative roles of thermal buoyancy, thermophoretic nanoparticle transport, and microorganism dynamics in shaping the basic-state structure, and they establish a foundation for future linear stability analysis of the system.

2. RESEARCH METHODS

2.1 Governing Equations

The governing equations for nanofluid bioconvection in a horizontal layer with gyrotactic microorganisms are adapted from Kuznetsov [12], building on Hill et al.'s foundational work [4] and the nanofluid model by Nield and Kuznetsov [40], which incorporates zero-nanoparticle flux boundary conditions. The model follows Kuznetsov [12] with several simplifying assumptions. The nanofluid suspension is considered dilute, allowing the neglect of microorganism interactions, and the fluid is assumed to be incompressible. Chemical reactions and particle aggregation are ignored. Nanoparticle transport accounts for both Brownian diffusion and thermophoresis, while microorganism motion follows gyrotactic behaviour driven by viscous and gravitational torques. Buoyancy effects due to temperature, concentration of nanoparticles, and density of microorganisms are included via the Boussinesq approximation. The fluid layer has a finite vertical depth, is horizontally infinite, and is bound by rigid, impermeable, thermally controlled surfaces.

The governing equations include continuity, momentum, thermal energy, conservation of nanoparticles, and conservation of microorganisms within the suspension [12]. In the following formulation, variables denoted with a bar represent dimensional quantities, and the vector $\bar{\mathbf{v}} = (\bar{u}, \bar{v}, \bar{w})$ denotes the components of nanofluid velocity in the x, y, and z directions.

$$\nabla \cdot \bar{\mathbf{v}} = 0, \tag{1}$$

$$\rho_{f0}\left(\frac{\partial \bar{\mathbf{v}}}{\partial \bar{t}} + \bar{\mathbf{v}} \cdot \nabla \bar{\mathbf{v}}\right) = -\nabla \bar{p} + \mu \nabla^2 \bar{\mathbf{v}} + \begin{bmatrix} \bar{\phi}\rho_{np} + (1-\bar{\phi})\rho_{f0} - \rho_{f0}\beta(\bar{T} - \bar{T}_c) + \\ (\rho_{np} - \rho_{f0})(\bar{\phi} - \bar{\phi}_0) + \bar{n}\bar{\theta}\Delta\rho \end{bmatrix}\mathbf{g}, \tag{2}$$

$$(\rho c)_f\left(\frac{\partial \bar{T}}{\partial \bar{t}} + \bar{\mathbf{v}} \cdot \nabla \bar{T}\right) = \nabla \cdot (k \nabla \bar{T}) + (\rho c)_{np}\left(D_B \nabla \bar{\phi} \cdot \nabla \bar{T} + D_T \frac{\nabla \bar{T} \cdot \nabla \bar{T}}{\bar{T}_c}\right), \tag{3}$$

$$\frac{\partial \bar{\phi}}{\partial \bar{t}} + \bar{\mathbf{v}} \cdot \nabla \bar{\phi} = \nabla \cdot \left[D_B \nabla \bar{\phi} + \frac{D_T}{\bar{T}_c} \nabla \bar{T}\right], \tag{4}$$

$$\frac{\partial \bar{n}}{\partial \bar{t}} = -\nabla \cdot \bar{\mathbf{j}}, \tag{5}$$

where $\bar{p}$ is the pressure, $\bar{t}$ is the time, and ρ is the density. The subscripts np, $f0$, and f refer to nanoparticles, base fluid, and nanofluid, respectively. Here, $\bar{T}$ is the nanofluid temperature, $\bar{T}_c$ is the temperature of the upper wall, $\bar{\phi}$ is the volume fraction of nanoparticle, $\bar{\phi}_0$ is the reference value of the nanoparticle volume fraction, β is the volumetric coefficient of thermal expansion of the base fluid, $\bar{n}$ is the concentration of gyrotactic microorganisms, $\bar{\theta}$ is the average volume of the microorganisms, $\Delta\rho = \rho_{cell} - \rho_{f0}$ represents the density difference between a microorganism cell and the base fluid, $\mathbf{g}$ is the vector of gravitational force, k is the thermal conductivity, and μ is the viscosity of the suspension. The symbols D_B and D_T are the Brownian and thermophoretic diffusion coefficients, respectively, c_f is the specific heat capacity for nanofluid, and c_{np} is the specific heat capacity for nanoparticles.

The term $\bar{\mathbf{j}}$ in Eq. (5) is defined as

$$\bar{\mathbf{j}} = \bar{n}\bar{\mathbf{v}} + \bar{n}W_c\hat{\mathbf{p}} - D_m \nabla \bar{n}, \tag{6}$$

which describes the behaviour of gyrotactic microorganisms inside a suspension, provided by Hill et al. [4]. The three terms on the right-hand side of Eq. (6) represents the total flux of microorganisms due to fluid convection, swimming movement driven by the microorganism's own propulsion, and diffusion, respectively. $W_c\hat{\mathbf{p}}$ is the vector denoting the microorganism's average swimming velocity relative to the nanofluid, where W_c is a constant while D_m is the diffusivity of microorganisms.

The physical model of this system is illustrated in Fig. 1. Here, H represents the height of the finite depth layer configuration. We consider a rigid-rigid boundaries configuration and assume that both the temperature and the volumetric fraction of the nanoparticles are constant on the upper and lower boundaries of suspension layer. At the bottom of the layer, the boundary conditions are

$$\bar{w}=0, \qquad \frac{\partial \bar{w}}{\partial \bar{z}}=0, \qquad \bar{T}=\bar{T}_h, \qquad D_B\frac{\partial \bar{\phi}}{\partial \bar{z}}+\frac{D_T}{\bar{T}_c}\frac{\partial \bar{T}}{\partial \bar{z}}=0, \qquad \bar{\mathbf{j}}\cdot\hat{\mathbf{k}}=0, \tag{7}$$

at $\bar{z}=0$, where $\bar{T}_h$ is the temperature of the lower layer. The unit vector $\hat{\mathbf{k}}$ represents the direction of the vertical axis, pointing upward. The boundary conditions for the upper layer are

$$\bar{w}=0, \qquad \frac{\partial \bar{w}}{\partial \bar{z}}=0, \qquad \bar{T}=\bar{T}_c, \qquad D_B\frac{\partial \bar{\phi}}{\partial \bar{z}}+\frac{D_T}{\bar{T}_c}\frac{\partial \bar{T}}{\partial \bar{z}}=0, \qquad \bar{\mathbf{j}}\cdot\hat{\mathbf{k}}=0. \tag{8}$$

at $\bar{z}=H$.

Hill et al. [4] noted that the upper boundary is unlikely to be entirely stress-free, even when exposed to air, because microorganisms tend to aggregate near the surface, forming a densely packed layer. Consequently, the no-slip condition is imposed at the upper wall. The boundary conditions in Eqs. (7) and (8) are adapted from Kuznetsov [12] with a minor adjustment to the nanoparticle volume fraction $\bar{\phi}$, in accordance with the zero-nanoparticle flux boundary formulation introduced by Nield and Kuznetsov [40]. The zero-nanoparticle flux boundary condition represents zero net nanoparticle flux at the impermeable boundaries. Physically, this means that nanoparticles cannot enter or leave the layer through the walls. Instead, the Brownian diffusion of nanoparticles is balanced by their thermophoretic migration induced by the temperature gradient. As a result, the boundaries only influence how nanoparticles are redistributed within the layer, rather than fixing their concentration at the walls.

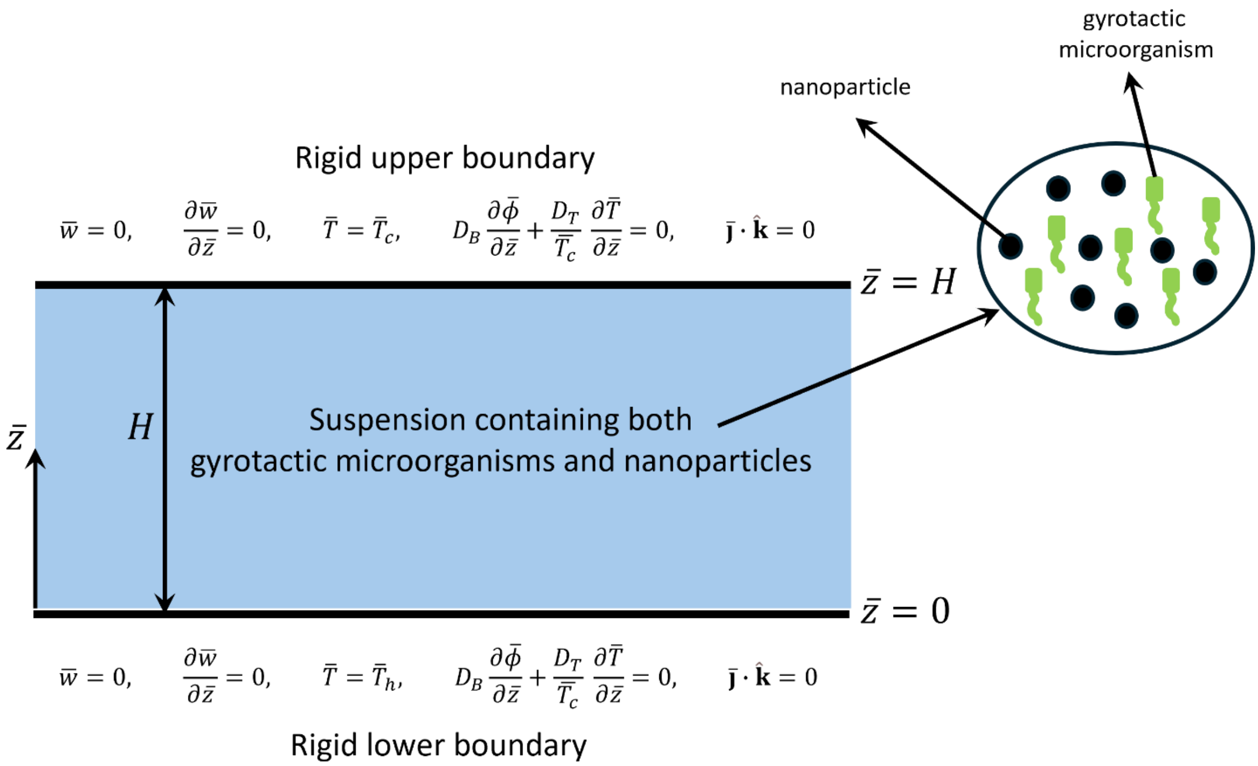

Figure 1. Physical Configuration and Coordinates for the Model.

2.2 Nondimensionalization

The variables that involved in Eqs. (1)-(8) are then nondimensionalized using appropriate characteristic scales adapted from Nield and Kuznetsov [40] and Kuznetsov [39]:

$$\begin{gathered} x=\frac{1}{H}\bar{x}, \qquad y=\frac{1}{H}\bar{y}, \qquad z=\frac{1}{H}\bar{z}, \qquad u=\frac{H}{\alpha_f}\bar{u}, \qquad v=\frac{H}{\alpha_f}\bar{v}, \qquad w=\frac{H}{\alpha_f}\bar{w}, \\ t=\frac{\alpha_f}{H^2}\bar{t}, \qquad p=\frac{H^2}{\mu\alpha_f}\bar{p}, \qquad \phi=\frac{\bar{\phi}-\bar{\phi}_0}{\bar{\phi}_0}, \qquad T=\frac{\bar{T}-\bar{T}_c}{\Delta T}, \qquad n=\frac{\bar{n}}{\bar{n}_{\mathrm{avg}}}, \end{gathered} \tag{9}$$

where $\alpha_f = k/(\rho c)_f$ refers to the thermal diffusivity of the nanofluid and $\Delta T = \bar{T}_h - \bar{T}_c$ is the temperature difference between two boundaries of lower and upper layers. Upon applying the dimensionless expressions Eq. (9), Eqs. (1)-(5) become

$$\nabla\cdot\mathbf{v}=0, \tag{10}$$

$$\frac{1}{\mathrm{Pr}}\left(\frac{\partial\mathbf{v}}{\partial t}+\mathbf{v}\cdot\nabla\mathbf{v}\right)=-\nabla p+\nabla^2\mathbf{v}-\mathrm{Rm}\,\hat{\mathbf{k}}+\mathrm{Ra}\,T\,\hat{\mathbf{k}}-\mathrm{Rn}\,\phi\,\hat{\mathbf{k}}-\frac{\mathrm{Rb}}{\mathrm{Lb}}n\,\hat{\mathbf{k}}, \tag{11}$$

$$\frac{\partial T}{\partial t}+\mathbf{v}\cdot\nabla T=\nabla^2 T+\frac{\mathrm{N_B}}{\mathrm{Le}}\nabla\phi\cdot\nabla T+\frac{\mathrm{N_A}\,\mathrm{N_B}}{\mathrm{Le}}\nabla T\cdot\nabla T, \tag{12}$$

$$\frac{\partial\phi}{\partial t}+\mathbf{v}\cdot\nabla\phi=\frac{1}{\mathrm{Le}}\nabla^2\phi+\frac{\mathrm{N_A}}{\mathrm{Le}}\nabla^2 T, \tag{13}$$

$$\frac{\partial n}{\partial t}=-\nabla\cdot\left(n\,\mathbf{v}+\frac{\mathrm{Q}}{\mathrm{Lb}}n\,\hat{\mathbf{p}}-\frac{1}{\mathrm{Lb}}\nabla n\right), \tag{14}$$

The dimensionless form of the boundary conditions Eqs. (7) and (8) now becomes

$$w=0, \qquad \frac{\partial w}{\partial z}=0, \qquad T=1, \qquad \frac{\partial\phi}{\partial z}+\mathrm{N_A}\frac{\partial T}{\partial z}=0, \qquad n=\frac{1}{\mathrm{Q}}\frac{dn}{dz}, \tag{15}$$

when $z = 0$, and

$$w=0, \qquad \frac{\partial w}{\partial z}=0, \qquad T=0, \qquad \frac{\partial\phi}{\partial z}+\mathrm{N_A}\frac{\partial T}{\partial z}=0, \qquad n=\frac{1}{\mathrm{Q}}\frac{dn}{dz}, \tag{16}$$

when $z = 1$.

In Eqs. (10)-(16), the dimensionless parameters are defined as follows:

$$\begin{gathered} \mathrm{Pr}=\frac{\mu}{\rho_{f0}\alpha_f}, \qquad \mathrm{Le}=\frac{\alpha_f}{D_B}, \qquad \mathrm{Lb}=\frac{\alpha_f}{D_m}, \qquad \mathrm{Q}=\frac{W_cH}{D_m}, \\ \mathrm{Ra}=\frac{\rho_{f0}g\beta H^3\Delta T}{\mu\alpha_f}, \qquad \mathrm{Rm}=\frac{\left[\rho_{np}\bar{\phi}_0+\rho_{f0}(1-\bar{\phi}_0)\right]gH^3}{\mu\alpha_f}, \\ \mathrm{Rn}=\frac{(\rho_{np}-\rho_{f0})\bar{\phi}_0 gH^3}{\mu\alpha_f}, \qquad \mathrm{Rb}=\frac{\Delta\rho g\bar{n}_{\mathrm{avg}}\bar{\theta}H^3}{\mu D_m}, \\ \mathrm{N_A}=\frac{D_T\Delta T}{D_B\bar{T}_c\bar{\phi}_0}, \qquad \mathrm{N_B}=\bar{\phi}_0\frac{(\rho c)_{np}}{(\rho c)_f}. \end{gathered} \tag{17}$$

Eq. (17) defines the physical parameters as follows: g represents the gravitational acceleration; Pr denotes the Prandtl number; Le is the Lewis number associated with Brownian diffusion of nanoparticles; Lb is the bioconvection Lewis number; Q corresponds to the bioconvection Péclet number; Ra, Rm, Rn, and Rb are the thermal, basic-density, nanoparticle concentration, and bioconvection Rayleigh numbers, respectively. The parameters $\mathrm{N_A}$ and $\mathrm{N_B}$ represent the modified diffusivity ratio and the modified particle-density increment.

2.3 Basic-State Equations

To analyse the underlying steady-state structure of the bioconvective nanofluid system, we begin by considering Eqs. (1) – (5) under the assumption of a quiescent basic state. In this configuration, the velocity field $\mathbf{v}$ is taken to be zero, and all dependent variables, namely temperature T, nanoparticle concentration ϕ, and microorganism density n are assumed to vary only in the vertical coordinate z, given by

$$\mathbf{v} = (u, v, w) = 0, \qquad p = p_b(z), \qquad T = T_b(z), \qquad \phi = \phi_b(z), \qquad n = n_b(z). \tag{18}$$

Upon disregarding both time and convective contributions, substitution of Eq. (18) into Eqs. (10)-(14) yields a system of coupled ordinary differential equations:

$$-\frac{dp_b(z)}{dz} - \mathrm{Rm} + \mathrm{Ra}\, T_b(z) - \mathrm{Rn}\, \phi_b(z) - \frac{\mathrm{Rb}}{\mathrm{Lb}} n_b(z) = 0, \tag{19}$$

$$\frac{d^2 T_b(z)}{dz^2} + \frac{\mathrm{N_B}}{\mathrm{Le}}\left(\frac{d\phi_b(z)}{dz}\right)\left(\frac{dT_b(z)}{dz}\right) + \frac{\mathrm{N_A}\,\mathrm{N_B}}{\mathrm{Le}}\left(\frac{dT_b(z)}{dz}\right)^2 = 0, \tag{20}$$

$$\frac{d^2\phi_b(z)}{dz^2} + \mathrm{N_A}\frac{d^2 T_b(z)}{dz^2} = 0, \tag{21}$$

$$\frac{dn_b(z)}{dz} - \mathrm{Q} n_b(z) = 0, \tag{22}$$

subject to the boundary conditions:

$$T_b = 1, \qquad \frac{d\phi_b}{dz} + \mathrm{N_A}\frac{dT_b}{dz} = 0, \qquad n_b = \frac{1}{\mathrm{Q}}\frac{dn_b}{dz}, \tag{23}$$

when $z = 0$, and

$$T_b = 0, \qquad \frac{d\phi_b}{dz} + \mathrm{N_A}\frac{dT_b}{dz} = 0, \qquad n_b = \frac{1}{\mathrm{Q}}\frac{dn_b}{dz}. \tag{24}$$

when $z = 1$.

Following the notation of Kuznetsov [39], the pressure gradient profile is expressed as negative, $-\frac{dp_b(z)}{dz}$, to reflect the direction of pressure variation along the vertical axis. Hence, the subsequent results will present $-p_b(z)$ for consistency.

3. RESULTS AND DISCUSSION

This section presents the analytical solutions of basic-state Eqs. (19)-(22) under the boundary conditions specified in Eqs. (23) and (24).

3.1 Analytical Solutions of Basic-State Equations

To obtain an analytical solution, we first integrate Eqs. (21) once and, using the boundary conditions in Eqs. (23) and (24), arrive at the following expression:

$$\frac{d\phi_b}{dz} + \mathrm{N_A}\frac{dT_b}{dz} = 0, \tag{25}$$

which has the same form as the boundary condition for ϕ_b in Eqs. (23) and (24). Rewrite Eq. (25) into this form:

$$\frac{d\phi_b}{dz} = -\mathrm{N_A}\frac{dT_b}{dz}, \tag{26}$$

Then. substitute Eq. (26) into Eq. (20). After simplifying it, we obtain:

$$\frac{d^2 T_b}{dz^2} = 0. \tag{27}$$

Eq. (27) has a general solution in the form of $C_1 z + C_2$. Applying the boundary conditions Eqs. (23) and (24), the exact solution for temperature profile is then obtained,

$$T_b(z) = 1 - z. \tag{28}$$

We now proceed to solve Eq. (25). The first derivative of Eq. (28) is simply -1. Substituting this value into Eq. (25), we obtain the following expression:

$$\frac{d\phi_b}{dz} = \mathrm{N_A}. \tag{29}$$

Thus, the solution of Eq. (29) is:

$$\phi_b(z) = \mathrm{N_A} z + \phi_0, \tag{30}$$

where the constant of integration ϕ_0 is the reference value of the nanoparticle volume fraction [40].

Integration of Eq. (22) yields the following result:

$$n_b(z) = C e^{\mathrm{Q}z}, \tag{31}$$

where the integration constant C is given by

$$C = \frac{\tilde{n}\,\mathrm{Q}}{e^{\mathrm{Q}} - 1}, \tag{32}$$

and $\tilde{n}$ is the mean concentration of microorganisms, follow the definition given by Kuznetsov [12],

$$\tilde{n} = \int_0^1 n_b(z)\,dz. \tag{33}$$

Kuznetsov [39] noted that $n_b(z)$ may be normalized so that its integral over the layer, $\int_0^1 n_b(z)\,dz$, equals unity (see Eq. (9)). This normalization ensures that the total number of microorganisms within the layer remains unchanged, whereas variations in $n_b(z)$ represent only changes in their spatial distribution. Thus, the exact solution for microorganisms' concentration can be written as:

$$n_b(z) = \frac{\mathrm{Q}\,e^{\mathrm{Q}z}}{e^{\mathrm{Q}} - 1}. \tag{34}$$

Finally, the pressure profile $-p_b$ can be acquired by substituting Eqs. (28), (30) and (34) into Eq. (19) and performing integration along $(0, z)$ domain of z-axis, we obtain:

$$-p_b(z) = \mathrm{Rm}\,z - \mathrm{Ra}\left(z - \frac{z^2}{2}\right) + \mathrm{Rn}\left(\frac{\mathrm{N_A} z^2}{2} + \phi_0\,z\right) + \frac{\mathrm{Rb}}{\mathrm{Lb}}\left(\frac{e^{\mathrm{Q}z} - 1}{e^{\mathrm{Q}} - 1}\right). \tag{35}$$

Since the present formulation employs the revised zero-nanoparticle flux boundary conditions proposed by Nield and Kuznetsov [40], the obtained temperature and nanoparticle concentration profiles are consistent with the corresponding results reported in [40] under the same boundary condition framework. In addition, the exact solution for microorganism concentration is consistent with that given by Kuznetsov [39], since the governing basic-state equation for gyrotactic microorganisms has the same form. Hence, the thermal, nanoparticle, and microorganism basic-state profiles each agree with the appropriate existing formulations. By contrast, the pressure profile $p_b(z)$ is formed from the combined contributions of these exact solutions through Eq. (19) and is therefore not expected to coincide exactly with results derived under different model assumptions or boundary-condition settings. Accordingly, the validity of the present pressure expression is confirmed by direct substitution into the reduced governing equations and by exact satisfaction of all imposed boundary conditions.

Moreover, the pressure values reported in the subsequent tables and figures are evaluated directly from the exact analytical expression in Eq. (35). Hence, the small percentage variations observed later reflect the true analytical sensitivity of the model under the chosen parameter values, rather than numerical approximation errors.

3.2 Estimation of the Values for Dimensionless Parameters

Before proceeding with the analysis of how the principal parameters influence the basic-state profiles, it is necessary to determine the representative values of the dimensionless parameters defined in Eq. (17).

Based on Buongiorno [10], the physical properties of the alumina–water nanofluid employed in this study are listed in Table 1.

Table 1. Values for Physical Parameters at 300K

Parameter	Value	Unit
$\bar{\phi}_0$	0.01	-
ρ_{f0}	10^3	$\mathrm{kg\ m^{-3}}$
ρ_{np}	4×10^3	$\mathrm{kg\ m^{-3}}$
$(\rho c)_{np}$	3.1×10^6	$\mathrm{J\ m^{-3}}$
$(\rho c)_f$	4×10^6	$\mathrm{J\ m^{-3}}$
α_f	2×10^{-7}	$\mathrm{m^2\ s^{-1}}$
D_B	4×10^{-11}	$\mathrm{m^2\ s^{-1}}$
D_T	6×10^{-11}	$\mathrm{m^2\ s^{-1}}$
μ	10^{-3}	Pa s
β	3.4×10^{-3}	$\mathrm{K^{-1}}$
$\bar{T}_c$	300	K
ΔT	1	K

Table 2 shows the estimate values of physical parameters for gyrotactic microorganisms, which we refer to Hill et al. [4] data for algae *Chlamydomonas nivalis*:

Table 2. Physical Parameters for Gyrotactic Microorganisms

Parameter	Value	Unit
D_m	5×10^{-8}	$\mathrm{m^2\ s^{-1}}$
W_c	10^{-4}	$\mathrm{m\ s^{-1}}$
$\Delta\rho$	50	$\mathrm{kg\ m^{-3}}$
$\bar{n}_{\mathrm{avg}}$	10^{12}	$\mathrm{cells\ m^{-3}}$
$\bar{\theta}$	5×10^{-16}	$\mathrm{m^3}$
H	2.5×10^{-3}	m

Using the physical quantities given in Table 2, the values of the dimensionless parameters in Eq. (17) are given by Table 3:

Table 3. Calculated Dimensionless Parameters

Parameter	Value
Pr	5.0
Le	5000
Lb	4.0
Q	5.0
Ra	2605.781250
Rm	789398.437500
Rn	22992.187500
Rb	76.640625
$\mathrm{N_A}$	0.50
$\mathrm{N_B}$	0.007750
ϕ_0	0

The value of ϕ_0 in Eq. (30) becomes zero after applying the nondimensionalization based on Eq. (9). Fig. 2 (a) shows the graphs of $T_b(z)$, and $\phi_b(z)$, Fig. 2 (b) presents the graph of $n_b(z)$ and Fig. 2 (c) presents the graph of $-p_b(z)$ for these parameter values. Figure 2 (a) shows that the temperature profile $T_b(z)$ decreases linearly from the lower boundary to the upper boundary, while the nanoparticle concentration profile $\phi_b(z)$ increases linearly with height. The linear increase in $\phi_b(z)$ is attributed to thermophoresis effect which drives nanoparticles away from the heated bottom wall ($z = 0$) toward the cooler top wall ($z = 1$). Fig. 2 (b) shows that the basic-state microorganism concentration $n_b(z)$ behaves monotonically with height and becomes sharply larger near the upper boundary due to its exponential dependence on z. This behaviour reflects the upward migration of gyrotactic microorganisms, leading to cell accumulation near the top of the layer [4]. Fig. 2 (c) shows that the basic-state pressure profile, $-p_b(z)$, increases almost linearly from the lower boundary to the upper boundary, attaining its maximum value at $z = 1$. These basic-state profiles highlight the distinct physical roles of heat transfer, nanoparticle transport, microorganism swimming, and hydrostatic pressure distribution in the finite-depth configuration. These Fig. 2 were produced using Python coding with the matplotlib library.

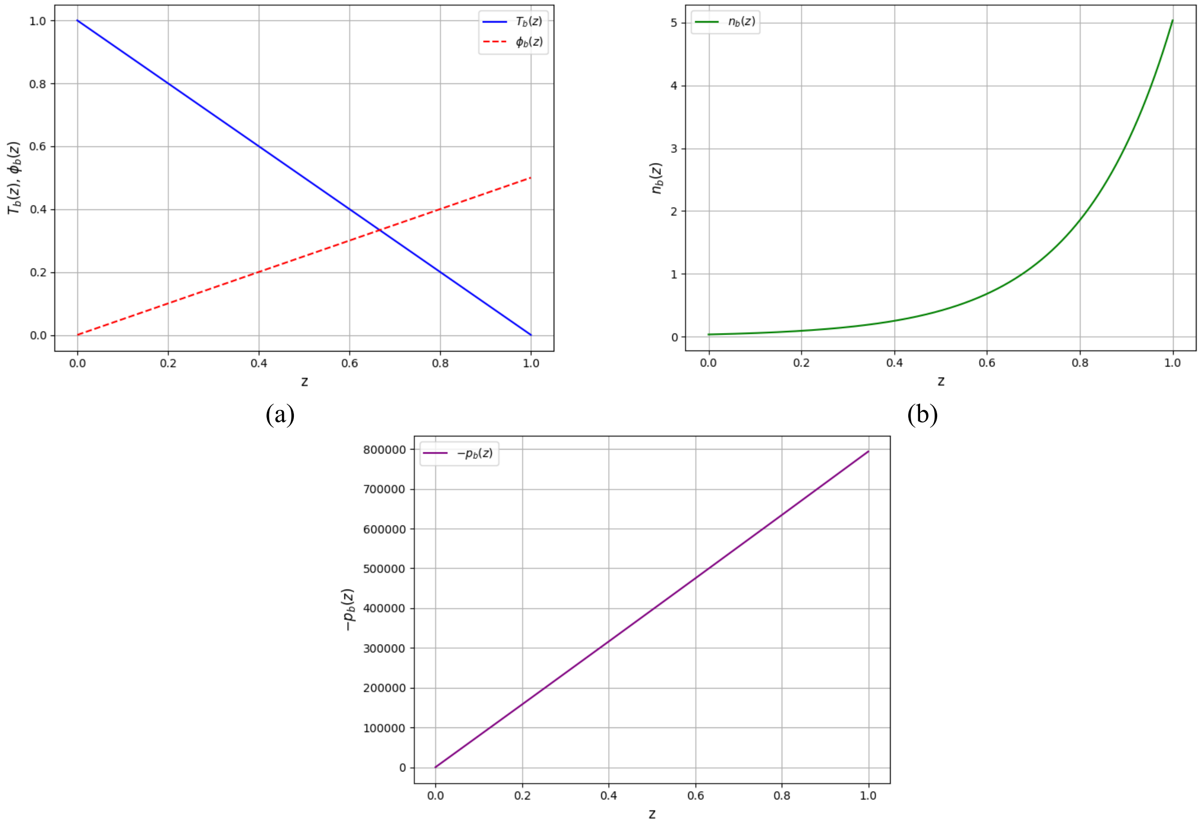

(c)

Figure 2. Basic-state Profiles for (a) $T_b(z)$ and $\phi_b(z)$; (b) $n_b(z)$; (c) $-p_b(z)$

In accordance with the methodology adopted by Kuznetsov [39], the base-state profiles are examined parametrically by varying the bioconvection Péclet number Q, the bioconvection Rayleigh number Rb, and the thermal Rayleigh number Ra. Overall, this parametric study is intended to distinguish the relative roles of microorganism swimming, microorganism-induced buoyancy, and thermal-thermophoretic effects in shaping the steady basic-state structure. In addition, we also vary the modified diffusivity ratio $\mathrm{N_A}$ to further explore its effects, as both Ra and $\mathrm{N_A}$ are directly influenced by temperature variation. In contrast, varying parameters such as $\mathrm{N_B}$, Rm, Rn, and Lb would require adopting different nanoparticles with distinct physical properties, adjusting the base state concentration ϕ_0, and selecting different types of microorganisms (in the case of Lb). However, increasing ϕ_0 beyond 0.01 is generally unrealistic for practical nanofluid applications, as Buongiorno [10] noted that most nanofluid studies maintain $\phi_0 < 0.05$ to preserve the dilute mixture assumption and ensure suspension stability.

3.3 Effects of Péclet Number Q

First, we examine different values of Q, which are 0.1, 1, and 10 while other parameters are set as fixed values (see Table 3). According to Kuznetsov [39], $\mathrm{Q} = 0.1$ refers to slowly swimming algae that has small W_c, $\mathrm{Q} = 1.0$ refers to intermediate swimmers that has intermediate W_c, and $\mathrm{Q} = 10$ refers to fast swimmers that has large W_c. Fig. 3 shows how microorganism concentration $n_b(z)$ changes with different values of Q, which measures swimming strength. For $\mathrm{Q} = 0.1$, the concentration is almost uniform. With $\mathrm{Q} = 1.0$, microorganisms start to gather near the top. For $\mathrm{Q} = 10$, the concentration rises sharply near the top boundary, meaning microorganisms strongly swim upward and accumulate there. Physically, this means that the Péclet number mainly controls the redistribution of microorganisms rather than the hydrostatic pressure field.

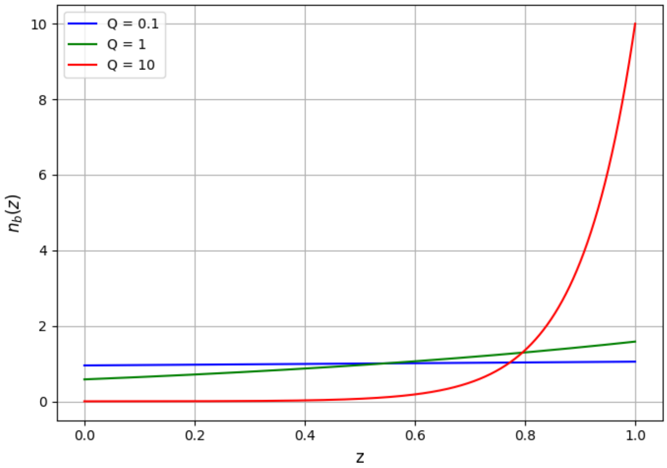

Figure 3. Effect of Q on $n_b(z)$

The changes in Q have a minimal effect on the pressure profile $-p_b(z)$, as shown in Table 4. As Q varies from 0.1, 1.0, and 10, the pressure values at each height remain almost unchanged, with percentage differences ranging from $10^{-4}\%$ to $10^{-3}\%$. The magnitude of this reduction is extremely small and indicates that the basic-state pressure is genuinely only weakly sensitive to variations in Q within the present parameter regime. This is because although Q significantly affects microorganism concentration $n_b(z)$, its impact on pressure is indirect and limited by the relatively small contribution of the pressure term involving $\frac{\mathrm{Rb}}{\mathrm{Lb}}\left(\frac{e^{\mathrm{Q}z}-1}{e^{\mathrm{Q}}-1}\right)$ in Eq. (35). Hence, the basic-state pressure may be regarded as effectively independent of the swimming strength parameter Q, with pressure remaining largely governed by other dominant terms such as the thermal and bulk buoyancy effects. At $z = 1$, the pressure value is the same for all Q because the Q-dependent contribution cancels out in the final expression of Eq. (35).

Table 4. $-\boldsymbol{p_b(z)}$ for different **Q** values

z	$-p_b(z)$			Percentage Change (%)	
	Q = 0.1	Q = 1.0	Q = 10	Q = 1.0 vs Q = 0.1	Q = 10 vs Q = 1.0
0.00	-0.0000	-0.0000	-0.0000	0	0
0.25	197143.4596	197142.0148	197138.8574	7.33×10^{-4}	2.33×10^{-3}
0.50	395168.4031	395166.2962	395159.1907	5.33×10^{-4}	2.33×10^{-3}
0.75	594074.8336	594073.0999	594062.2165	2.92×10^{-4}	2.12×10^{-3}
1.00	793862.7539	793862.7539	793862.7539	0	0

3.4 Effects of Bioconvection Rayleigh Number Rb

Next, we examine the effects of bioconvection Rayleigh number Rb on the pressure profile $-p_b(z)$. As mentioned by Kuznetsov [39], Rb can be controlled by adjusting the cell concentration within the nanofluid suspension. We consider three different values of Rb: 0, 50, and 100, following the approach of Kuznetsov [39], while keeping all other parameters fixed as previously defined (see Table 3). It is observed from Table 5, as the value of Rb increases, the pressure $-p_b(z)$ at each height z becomes marginally larger. This is due to the stronger buoyancy effect from the microorganisms, represented by $\frac{\mathrm{Rb}}{\mathrm{Lb}}\left(\frac{e^{\mathrm{Q}z}-1}{e^{\mathrm{Q}}-1}\right)$ in Eq. (35), which contributes to an increase in fluid pressure throughout the layer. In other words, a larger microorganism concentration effect leads to a modest strengthening of the hydrostatic pressure field through microorganism-induced buoyancy.

However, similar to the variations observed for Q, the corresponding percentage changes ranging from $10^{-4}\%$ to $10^{-3}\%$, indicating that the effect is extremely small in magnitude and shows that the basic-state pressure is also weakly sensitive to variations in Rb over the present range. The overall trend of pressure increasing with height remains unchanged in all cases.

Table 5. $-p_b(z)$ for different **Rb** values

z	$-p_b(z)$			Percentage Change (%)	
	Rb = 0	Rb = 50	Rb = 100	Rb = 50 vs Rb = 0	Rb = 100 vs Rb = 0
0.00	-0.0000	-0.0000	-0.0000	0	0
0.25	197138.8477	197139.0588	197139.2700	1.07×10^{-4}	2.14×10^{-4}
0.50	395159.0625	395160.0107	395160.9590	2.40×10^{-4}	4.80×10^{-4}
0.75	594060.6445	594064.1653	594067.6861	5.93×10^{-4}	1.185×10^{-3}
1.00	793843.5938	793856.0938	793868.5938	1.575×10^{-3}	3.149×10^{-3}

3.5 Effects of Thermal Rayleigh Number Ra and Modified Diffusivity Ratio $\mathrm{N_A}$

Furthermore, we examine the effect of the thermal Rayleigh number Ra and modified diffusivity ratio $\mathrm{N_A}$ on the pressure profile $-p_b(z)$. Kuznetsov [39] pointed out that Ra can be controlled by changing the temperature difference between two boundaries of upper and lower layers (ΔT term on Ra in Eq. (17)). Similarly, $\mathrm{N_A}$ is also influenced by temperature difference. We consider three different scenarios with temperature differences of 1K, 2K, and 3K. Thus, this corresponds to three different Ra values, which are 2605.7813, 5211.5625, and 7817.3438 and three different $\mathrm{N_A}$ values of 0.5, 1.0, and 1.5, respectively, while the other parameters are kept fixed as previously defined (see Table 3).

Table 6 shows that the variations in the Rayleigh number Ra and the modified diffusivity ratio $\mathrm{N_A}$ produce the most noticeable changes in the pressure profile when compared with the cases of Q and Rb. This indicates that thermal buoyancy and thermophoretic transport play the dominant role in determining the steady basic-state pressure distribution. Physically, a larger temperature difference strengthens the thermal driving force across the layer, while a larger $\mathrm{N_A}$ enhances the contribution of thermophoretic nanoparticle transport. As a result, the pressure profile becomes more strongly affected by thermal and nanoparticle transport mechanisms than by microorganism swimming alone. Although the response is not strictly uniform at every vertical position, the overall pressure variation becomes increasingly pronounced as the temperature difference increases. Nevertheless, the pressure profiles retain an approximately linear growth with respect to z, which is characteristic of the basic state behaviour under steady nanofluid bioconvection conditions.

Table 6. $-p_b(z)$ for different **Ra** and $\mathbf{N_A}$ values

z	$-p_b(z)$			Percentage Change (%)	
	$\Delta T = 1\text{K}$ Ra = 2605.7813 $\mathrm{N_A} = 0.5$	$\Delta T = 2\text{K}$ Ra = 5211.5625 $\mathrm{N_A} = 1.0$	$\Delta T = 3\text{K}$ Ra = 7817.3438 $\mathrm{N_A} = 1.5$	$\Delta T = 1\text{K}$ vs $\Delta T = 2\text{K}$	$\Delta T = 1\text{K}$ vs $\Delta T = 3\text{K}$
0.00	-0.0000	-0.0000	-0.0000	0	0
0.25	197139.1713	196928.4096	196717.6479	-1.07×10^{-1}	-2.14×10^{-1}
0.50	395160.5160	395620.3597	396080.2035	1.16×10^{-1}	2.33×10^{-1}
0.75	594066.0413	596077.8577	598089.6741	3.39×10^{-1}	6.77×10^{-1}
1.00	793862.7539	798307.9102	802753.0664	5.60×10^{-1}	1.12

In short, the results indicate that the steady hydrostatic pressure field is governed mainly by thermal buoyancy and thermophoretic nanoparticle transport, whereas microorganism swimming primarily controls the vertical redistribution and accumulation of cells within the layer.

4. CONCLUSION

This study presented a basic-state analysis of nanofluid bioconvection with gyrotactic microorganisms under zero-nanoparticle flux boundary conditions proposed by Nield and Kuznetsov [40]. The governing equations for the problem were nondimensionalized and solved analytically under the assumption of a quiescent (zero-velocity) basic state. The focus of this study is investigating how key physical parameters affect the pressure profile within the bioconvective nanofluid in a finite-depth configuration.

Overall, the results suggest that the steady basic-state structure is governed primarily by thermal and thermophoretic effects, while microbial swimming primarily affects the spatial redistribution of microorganisms. Physically, this indicates that microorganism activity plays a more significant role in concentration patterning than in modifying the background hydrostatic pressure field under steady conditions. The swimming strength parameter Q significantly affects microorganism accumulation near the top boundary but has minimal influence on the pressure profile. Similarly, increasing the bioconvection Rayleigh number Rb slightly raises the fluid pressure as it amplifies microorganism-induced buoyancy. In contrast, both the thermal Rayleigh number Ra and the modified diffusivity ratio N_A lead to noticeable pressure increases, hence, enhance buoyancy-driven convection and thermophoretic effects. The pressure profile remains nearly linear in all cases, consistent with the nature of the steady basic state.

The present findings provide useful physical insight into the role of zero-nanoparticle flux boundary conditions in finite-depth nanofluid bioconvection. In particular, the analytical basic-state solutions obtained here establish a foundation for future linear stability analysis, where the onset of convection, critical instability conditions, and possible pattern formation can be investigated under zero-nanoparticle flux boundary conditions.

Author Contributions

Ming Hui Lim: Modelling, Methodology, Software, Data Curation, Visualization, Writing-Original Draft. Yian Yian Lok: Conceptualization, Resources, Methodology, Validation, Writing-Review and Editing. Syakila Ahmad: Validation, Writing-Review and Editing. Norshafira Ramli: Writing-Review and Editing. Anuar Ishak: Resources, Validation, Writing-Review and Editing. All authors discussed the results, contributed to the manuscript's preparation, and approved the final version of publication.

Funding Statement

This research is supported by Fundamental Research Grant Scheme (FRGS) from Ministry of Higher Education Malaysia (Project Code: FRGS/1/2024/STG06/USM/02/10).

Acknowledgment

Special thanks are also extended to Universiti Sains Malaysia for providing institutional support throughout this project.

Declarations

The authors declare no conflict of interest.

Declaration of Generative AI and AI-assisted technologies

The authors declare that no generative AI or AI-assisted technologies were used in the preparation of this manuscript, including for writing, editing, data analysis, or the creation of tables and figures.

REFERENCES

[1] M. A. Bees, "ADVANCES IN BIOCONVECTION," *Annu. Rev. Fluid Mech.*, vol. 52, pp. 449–476, 2020. doi: https://doi.org/10.1146/annurev-fluid-010518-040558.

[2] H. W. T. Wager, "VII. ON THE EFFECT OF GRAVITY UPON THE MOVEMENTS AND AGGREGATION OF EUGLENA VIRIDIS, EHRB., AND OTHER MICRO-ORGANISMS," *Philosophical Transactions of the Royal Society B - Biological Sciences*, vol. 201, no. 274–281, pp. 333–390, 1911. doi: https://doi.org/10.1098/rstb.1911.0007.

[3] J. R. Platt, "'BIOCONVECTION PATTERNS' IN CULTURES OF FREE-SWIMMING ORGANISMS," *Science (1979)*, vol. 133, no. 3466, pp. 1766–1767, 1961. doi: https://doi.org/10.1126/science.133.3466.1766.

[4] N. A. Hill, T. J. Pedley, and J. O. Kessler, "GROWTH OF BIOCONVECTION PATTERNS IN A SUSPENSION OF GYROTACTIC MICRO-ORGANISMS IN A LAYER OF FINITE DEPTH," *J Fluid Mech*, vol. 208, pp. 509–543, 1989. doi: https://doi.org/10.1017/S0022112089002922.

[5] E. O. Ige, I. F. Odesola, S. B. Ayedun, and O. M. Ilori, "MAGNETO-ROTATIONAL AUGMENTATION OF BIOCONVECTIVE TRANSPORT IN PLASMA-NANOFLUID FLOWING THROUGH A PENETRABLE SPINNING DISC," *Journal of Engineering (United Kingdom)*, vol. 2022, 2022. doi: https://doi.org/10.1155/2022/3499192.

[6] K. Naganthran, M. F. Md Basir, T. Thumma, E. O. Ige, R. Nazar, and I. Tlili, "SCALING GROUP ANALYSIS OF BIOCONVECTIVE MICROPOLAR FLUID FLOW AND HEAT TRANSFER IN A POROUS MEDIUM," *J Therm Anal Calorim*, vol. 143, no. 3, pp. 1943–1955, 2021. doi: https://doi.org/10.1007/s10973-020-09733-5.

[7] N. Biswas, D. K. Mandal, N. K. Manna, and A. C. Benim, "ENHANCED ENERGY AND MASS TRANSPORT DYNAMICS IN A THERMO-MAGNETO-BIOCONVECTIVE POROUS SYSTEM CONTAINING OXYTACTIC BACTERIA AND NANOPARTICLES: CLEANER ENERGY APPLICATION," *Energy*, vol. 263, 2023. doi: https://doi.org/10.1016/j.energy.2022.125775

[8] S. U. Choi and J. A. Eastman, "ENHANCING THERMAL CONDUCTIVITY OF FLUIDS WITH NANOPARTICLES (NO. ANL/MSD/CP-84938; CONF-951135-29)," United States, 1995.

[9] R. K. Tiwari and M. K. Das, "HEAT TRANSFER AUGMENTATION IN A TWO-SIDED LID-DRIVEN DIFFERENTIALLY HEATED SQUARE CAVITY UTILIZING NANOFLUIDS," *Int J Heat Mass Transf*, vol. 50, no. 9–10, pp. 2002–2018, 2007. doi: https://doi.org/10.1016/j.ijheatmasstransfer.2006.09.034.

[10] J. Buongiorno, "CONVECTIVE TRANSPORT IN NANOFLUIDS," *J Heat Transfer*, vol. 128, no. 3, pp. 240–250, 2006. https://doi.org/10.1115/1.2150834.

[11] D. A. Nield and A. V Kuznetsov, "THE ONSET OF CONVECTION IN A HORIZONTAL NANOFLUID LAYER OF FINITE DEPTH," *European Journal of Mechanics - B/Fluids*, vol. 29, no. 3, pp. 217–223, 2010. doi: https://doi.org/10.1016/j.euromechflu.2010.02.003.

[12] A. V Kuznetsov, "THE ONSET OF NANOFLUID BIOCONVECTION IN A SUSPENSION CONTAINING BOTH NANOPARTICLES AND GYROTACTIC MICROORGANISMS," *International Communications in Heat and Mass Transfer*, vol. 37, no. 10, pp. 1421–1425, 2010. doi: https://doi.org/10.1016/j.icheatmasstransfer.2010.08.015.

[13] M. Ben Henda *et al.*, "APPLICATIONS OF ACTIVATION ENERGY ALONG WITH THERMAL AND EXPONENTIAL SPACE-BASED HEAT SOURCE IN BIOCONVECTION ASSESSMENT OF MAGNETIZED THIRD GRADE NANOFLUID OVER STRETCHED CYLINDER/SHEET," *Case Studies in Thermal Engineering*, vol. 26, 2021. doi: https://doi.org/10.1016/j.csite.2021.101043.

[14] Z. Hussain, M. M. Alam, A. A. Pasha, W. A. Khan, M. Ali, and A. I. Khan, "GYROTATIC MICROORGANISMS ANALYSIS FOR RADIATIVE 3D CARREAU NANOFLUID FLOW CONFIGURED BY ACTIVATION ENERGY AND VISCOUS DISSIPATION," *Thermal Science and Engineering Progress*, vol. 42, 2023. doi: https://doi.org/10.1016/j.tsep.2023.101898.

[15] N. Anjum, W. A. Khan, M. Azam, M. Ali, M. Waqas, and I. Hussain, "SIGNIFICANCE OF BIOCONVECTION ANALYSIS FOR THERMALLY STRATIFIED 3D CROSS NANOFLUID FLOW WITH GYROTACTIC MICROORGANISMS AND ACTIVATION ENERGY ASPECTS," *Thermal Science and Engineering Progress*, vol. 38, 2023. doi: https://doi.org/10.1016/j.tsep.2022.101596.

[16] K. A. M. Alharbi *et al.*, "NUMERICAL SOLUTION OF MAXWELL-SUTTERBY NANOFLUID FLOW INSIDE A STRETCHING SHEET WITH THERMAL RADIATION, EXPONENTIAL HEAT SOURCE/SINK, AND BIOCONVECTION," *International Journal of Thermofluids*, vol. 18, p. 100339, 2023. doi: https://doi.org/10.1016/j.ijft.2023.100339.

[17] H. U. Rasheed, Q. Shah, S. Latif, T. Abbas, and A. Ali. "OPTIMIZATION OF HEAT TRANSFER IN SUTTERBY NANOFLUID FLOW DRIVEN BY A FLEXIBLE SURFACE WITH GYROTACTIC MICROORGANISM AND ACTIVATION ENERGY," *ZAMM - Journal of Applied Mathematics and Mechanics / Zeitschrift Für Angewandte Mathematik Und Mechanik*, vol. 106, no. 2, 2026. doi: https://doi.org/10.1002/zamm.70345.

[18] K. Batool *et al.*, "AN INVESTIGATION OF HEAT TRANSFER AND OPTIMIZATION OF ENTROPY IN BIO-CONVECTIVE FLOW OF EYRING-POWELL NANOMATERIAL WITH GYROTACTIC MICROORGANISMS," *Case Studies in Thermal Engineering*, vol. 61, p. 104903, 2024. doi: https://doi.org/10.1016/j.csite.2024.104903.

[19] W. A. Khan, "DYNAMICS OF GYROTACTIC MICROORGANISMS FOR MODIFIED EYRING POWELL NANOFLUID FLOW WITH BIOCONVECTION AND NONLINEAR RADIATION ASPECTS," *Waves in Random and Complex Media*, vol. 36, no. 2, pp. 2157–2167, 2026. doi: https://doi.org/10.1080/17455030.2023.2168086.

[20] Z. Khan *et al.*, "NUMERICAL STUDY OF HYDROMAGNETIC BIOCONVECTION FLOW OF MICROPOLAR NANOFLUID PAST AN INCLINED STRETCHING SHEET IN A POROUS MEDIUM WITH GYROTACTIC MICROORGANISM," *J Comput Sci*, vol. 78, p. 102256, 2024. doi: https://doi.org/10.1016/j.jocs.2024.102256.

[21] M. Azam, "NON-LINEAR RADIATIVE HEAT FLUX OF WILLIAMSON NANOFLUID WITH GYROTACTIC MICROORGANISMS, ACTIVATION ENERGY AND BIOCONVECTION," *Waves in Random and Complex Media*, vol. 35, no. 7, pp. 14512–14534, 2026. doi: https://doi.org/10.1080/17455030.2022.2149883.

[22] A. K. Sarma and D. Sarma, "UNSTEADY MAGNETOHYDRODYNAMIC BIOCONVECTION CASSON FLUID FLOW IN PRESENCE OF GYROTACTIC MICROORGANISMS OVER A VERTICALLY STRETCHED SHEET," *Numerical Heat Transfer, Part A: Applications*, vol. 87, no. 1, 2026. doi: https://doi.org/10.1080/10407782.2024.2389338.

[23] A. Ali and B. Sarkar, "THERMODYNAMIC OPTIMIZATION OF BIOCONVECTIVE JEFFREY NANOFLUID–MICROORGANISM SYSTEMS IN MHD FLOW OVER STRETCHING CYLINDERS," *The European Physical Journal Plus*, vol. 141, no. 3, p. 214, 2026. doi: https://doi.org/10.1140/epjp/s13360-026-07448-4.

[24] H. A. Ghazwani, "MELTING HEAT TRANSPORT ANALYSIS FOR BIOCONVECTIVE RHEOLOGICAL NANOFLUID FLOW SUBJECT TO GYROTACTIC MICROORGANISM'S," *Case Studies in Thermal Engineering*, vol. 70, p. 106102, 2025. doi: https://doi.org/10.1016/j.csite.2025.106102.

[25] U. Arif and M. Nawaz, "NUMERICAL STUDY OF MOTILE GYROTACTIC MICRO-ORGANISMS IN HYBRID NANO-MAXWELL FLUID WITH MASS AND HEAT TRANSFER," *Waves in Random and Complex Media*, vol. 35, no. 7, pp. 13501–13517, 2026. doi: https://doi.org/10.1080/17455030.2022.2142319.

[26] I. Patgiri, B. S. Goud, H. Maaitah, and M. Y. Mustafa, "MAXWELL FLUID FLOW WITH GYROTACTIC MICROORGANISMS: EFFECTS OF SUCTION REYNOLDS NUMBER, ACTIVATION ENERGY, AND NONLINEAR HEAT RADIATION," *International Journal of Thermofluids*, vol. 32, p. 101560, 2026. doi: https://doi.org/10.1016/j.ijft.2026.101560.

[27] A. Hamid, U. Mehtab, and N. Farooq, "COMPUTATIONAL ANALYSIS FOR BIOCONVECTION FLOW OF NANOFLUID ALONG A BIDIRECTIONAL SURFACE CONTAINING GYROTACTIC MICROORGANISMS EMBEDDED IN A DARCY-FORCHHEIMER POROUS MEDIUM," *International Journal of Thermofluids*, vol. 26, p. 101059, 2025. doi: https://doi.org/10.1016/j.ijft.2025.101059.

[28] A. V. Kuznetsov and A. A. Avramenko, "EFFECT OF SMALL PARTICLES ON THIS STABILITY OF BIOCONVECTION IN A SUSPENSION OF GYROTACTIC MICROORGANISMS IN A LAYER OF FINITE DEPTH," *International Communications in Heat and Mass Transfer*, vol. 31, no. 1, pp. 1–10, 2004. doi: https://doi.org/10.1016/S0735-1933(03)00196-9.

[29] A. V. Kuznetsov and P. Geng, "THE INTERACTION OF BIOCONVECTION CAUSED BY GYROTACTIC MICRO-ORGANISMS AND SETTLING OF SMALL SOLID PARTICLES," *Int J Numer Methods Heat Fluid Flow*, vol. 15, no. 4, pp. 328–347, 2005. doi: https://doi.org/10.1108/09615530510590597.

[30] A. V Kuznetsov, "THE ONSET OF BIOCONVECTION IN A SUSPENSION OF GYROTACTIC MICROORGANISMS IN A FLUID LAYER OF FINITE DEPTH HEATED FROM BELOW," *International Communications in Heat and Mass Transfer*, vol. 32, no. 5, pp. 574–582, 2005. doi: https://doi.org/10.1016/j.icheatmasstransfer.2004.10.021.

[31] D. A. Nield and A. V. Kuznetsov, "THE ONSET OF BIO-THERMAL CONVECTION IN A SUSPENSION OF GYROTACTIC MICROORGANISMS IN A FLUID LAYER: OSCILLATORY CONVECTION," *International Journal of Thermal Sciences*, vol. 45, no. 10, pp. 990–997, 2006. doi: https://doi.org/10.1016/j.ijthermalsci.2006.01.007.

[32] Y. D. Sharma and V. Kumar, "THE EFFECT OF HIGH-FREQUENCY VERTICAL VIBRATION IN A SUSPENSION OF GYROTACTIC MICRO-ORGANISMS," *Mech Res Commun*, vol. 44, pp. 40–46, 2012. doi: https://doi.org/10.1016/j.mechrescom.2012.06.001.

[33] A. K. Kushwaha, Y. D. Sharma, and S. Saini, "IMPACT OF VERTICAL VIBRATION AND GYROTACTIC MICROORGANISMS ON STABILITY OF THERMO-BIOCONVECTION," *Mech Res Commun*, vol. 116, p. 103769, 2021. doi: https://doi.org/10.1016/j.mechrescom.2021.103769.

[34] A. A. Avramenko and A. V. Kuznetsov, "THE ONSET OF BIO-THERMAL CONVECTION IN A SUSPENSION OF GYROTACTIC MICROORGANISMS IN A FLUID LAYER WITH AN INCLINED TEMPERATURE GRADIENT," *Int J Numer Methods Heat Fluid Flow*, vol. 20, no. 1, pp. 111–129, 2010. doi: https://doi.org/10.1108/09615531011008154.

[35] K. Kaur, M. Danesh, and M. Arora, "EFFECT OF MICROORGANISMS ON THE STABILITY ANALYSIS IN MAGNETIC NANOFLUIDS," in *Journal of Physics: Conference Series*, IOP Publishing Ltd, p. 12008, 2021. doi: https://doi.org/10.1088/1742-6596/1849/1/012008.

[36] M. Arora, M. Danesh, and M. Kumar Sharma, "EFFECT OF ROTATION ON THE ONSET OF CONVECTION IN MAGNETIC NANOFLUIDS CONTAINING GYROTACTIC MICROORGANISMS," *J Phys Conf Ser*, vol. 2844, p. 12006, 2024. doi: https://doi.org/10.1088/1742-6596/2844/1/012006.

[37] E. N. Lorenz, "DETERMINISTIC NONPERIODIC FLOW," *Journal of atmospheric sciences*, vol. 20, no. 2, pp. 130–141, 1963. doi: https://doi.org/10.1175/1520-0469(1963)020<0130:DNF>2.0.CO;2.

[38] A. A. Avramenko, Y. Y. Kovetska, and I. V. Shevchuk, "LORENZ APPROACH FOR ANALYSIS OF BIOCONVECTION INSTABILITY OF GYROTACTIC MOTILE MICROORGANISMS," *Chaos Solitons Fractals*, vol. 166, p. 112957, 2023. doi: https://doi.org/10.1016/j.chaos.2022.112957.

[39] A. V. Kuznetsov, "NANOFLUID BIO-THERMAL CONVECTION: SIMULTANEOUS EFFECTS OF GYROTACTIC AND OXYTACTIC MICRO-ORGANISMS," *Fluid Dyn Res*, vol. 43, no. 5, p. 55505, 2011. doi: https://doi.org/10.1088/0169-5983/43/5/055505.

[40] D. A. Nield and A. V. Kuznetsov, "THE ONSET OF CONVECTION IN A HORIZONTAL NANOFLUID LAYER OF FINITE DEPTH: A REVISED MODEL," *Int J Heat Mass Transf*, vol. 77, pp. 915–918, 2014. doi: https://doi.org/10.1016/j.ijheatmasstransfer.2014.06.020.